

Seasonal Variations of CO₂, CH₄, N₂O and CO in the Mid-Troposphere over the Western North Pacific Observed Using a C-130H Cargo Aircraft

Yosuke NIWA, Kazuhiro TSUBOI, Hidekazu MATSUEDA, Yousuke SAWA

Oceanography and Geochemistry Research Department, Meteorological Research Institute, Tsukuba, Japan

Toshinobu MACHIDA

Center for Global Environmental Research, National Institute for Environmental Studies, Tsukuba, Japan

Masamichi NAKAMURA, Taro KAWASATO, Kazuyuki SAITO, Shinya TAKATSUJI,
Kentaro TSUJI, Hidehiro NISHI, Koshiro DEHARA, Yusuke BABA, Daisuke
KUBOIKE, Shohei IWATSUBO, Hidehiro OHMORI, and Yoshikazu HANAMIYA

Japan Meteorological Agency, Tokyo, Japan

(Manuscript received 28 March 2013, in final form 4 October 2013)

Abstract

Seasonal variations of carbon dioxide (CO₂), methane (CH₄), carbon monoxide (CO), and nitrous oxide (N₂O), in the mid-troposphere over the western North Pacific, are investigated using air samples collected onboard a C-130H aircraft. These samples were obtained between Atsugi Base (35.45°N, 139.45°E) and Minamitorishima (MNM; 24.28°N, 153.98°E), once a month, from September 2010 to September 2012. Increasing trends of CO₂ and N₂O and large variability of CH₄ and CO (at approximately 6 km) have been found. During summer, concentrations of CH₄ and CO were found to increase with height over MNM. High concentrations of CH₄ were persistently observed in the mid-troposphere throughout the observation period. The average enhancement ratios of CH₄ to CO above background levels ($\Delta\text{CH}_4/\Delta\text{CO}$) were 0.47 and 1.2 ppb/ppb for winter–spring and summer–fall, respectively. The results suggested that the high CH₄ concentrations originated primarily from fossil fuel combustions in winter–spring, while there could be an additional contribution from increased biogenic sources during summer–fall. Because a surface station in MNM rarely observed the summer–fall high CH₄ concentration values in the mid-troposphere, the aircraft measurements could provide a powerful constraint on the CH₄ emission estimates for Asia, in addition to that provided by the surface measurements. This aircraft measurement program is regularly conducted for the long-term monitoring of the greenhouse gases in the mid-troposphere, and it has a significant role for filling the data gap of the existing measurement network.

Keywords greenhouse gases; aircraft observation; mid-troposphere

Corresponding author: Yosuke Niwa, Oceanography and Geochemistry Research Department, Meteorological Research Institute, 1-1 Nagamine, Tsukuba, Ibaraki 305-0052, Japan
E-mail: yniwa@mri-jma.go.jp
©2014, Meteorological Society of Japan

1. Introduction

The monitoring of atmospheric greenhouse gases (GHGs), such as carbon dioxide (CO₂), methane (CH₄), and nitrous oxide (N₂O), over Asia has become an increasingly important scientific activity because

of rapidly growing anthropogenic emissions of these gases by economically growing Asian countries. In recent years, for example, China has turned out to be the largest anthropogenic CO₂ emitter in the world, surpassing the United States (Gregg et al. 2008; Peters et al. 2012). In addition to fossil fuel emissions, there also exist other strong anthropogenic GHG emission sources, such as CH₄ from livestock and rice cultivation and N₂O from agricultural land (Streets et al. 2003; Ohara et al. 2007; Huang et al. 2008). Asia also emits large amounts of natural GHGs such as CH₄ from wetlands and/or biomass burning (Ito and Inatomi 2012; van der Werf et al. 2010). Many of these sources are quite sensitive to climate change and so are strong driving forces of seasonal and interannual variations of atmospheric GHGs. Thus, there is a strong need to obtain better emission estimates of these gases by reducing uncertainties; to achieve this, spatially and temporally dense observational networks are required.

Over the East Asian continent, there still exist only a few GHG monitoring sites (e.g., Zhou et al. 2003, 2004). However, on the downwind side of the East Asian continent, i.e., around the Far East Asia and the western Pacific regions, there are several surface monitoring sites that continuously monitor atmospheric concentrations of GHGs and other trace gases (Sawa et al. 2007; Tanimoto et al. 2008; Tohjima et al. 2002, 2010; Wada et al. 2007, 2011; Turnbull et al. 2011; Zhu et al. 2012). In addition to these, there are shipboard measurements in the western Pacific areas (Tohjima et al. 2005; Yashiro et al. 2009; Terao et al. 2011; Nara et al. 2011), as well as measurements in the free troposphere using passenger aircraft (Nakazawa et al. 1991, 1993; Matsueda et al. 2002). Some of these data have been widely used to estimate GHG emissions in various inverse modeling studies (e.g., Gurney et al. 2002; Patra et al. 2005). Recently, a major aircraft measurement project named Comprehensive Observation Network for Trace gases by Airliner (CONTRAIL) has provided many CO₂ concentration profiles in the horizontal in the upper troposphere and in the vertical over tens of airports (Machida et al. 2008; Matsueda et al. 2008; Sawa et al. 2008, 2012; Shirai et al. 2012). In forward and inverse modeling studies, the CONTRAIL CO₂ data were found to provide additional constraints on flux estimation to those obtained by employing just the surface measurements (Patra et al. 2011; Niwa et al. 2011, 2012).

There is, however, a significant lack of long-term monitoring (spatially and temporally) of GHG concentrations in the mid-troposphere over the western Pacific region. In the past, several intensive observa-

tion campaigns using research aircraft revealed strong outflow of Asian pollutants in the mid-troposphere (e.g., Machida et al. 2002; Jacob et al. 2003; Sawa et al. 2004), and their long-range transport processes were investigated by three-dimensional model simulations (e.g., Liang et al. 2004). These campaign-style measurements were conducted for only short time periods, with focus on the winter–spring. However, during summer–fall, high CH₄ concentration events associated with Asian outflows are often captured by CONTRAIL in the upper troposphere over the western North Pacific (Matsueda and Inoue 1996; Umezawa et al. 2012; Schuck et al. 2012). It is suggested that we are missing some important transport and chemical transformation processes in the mid-troposphere because of very few observations over the region.

Since the mid of 2010, the Japan Meteorological Agency (JMA) has been conducting regular GHG observations in the mid-troposphere over the western North Pacific region by sampling air in flasks onboard a C-130H cargo aircraft (Tsuboi et al. 2013). In this paper, we present seasonal variations of CO₂, CH₄, N₂O, and carbon monoxide (CO) by analyzing measurements of the JMA aircraft observation. The length of the measurement record used in this study was two years. Results in the mid-troposphere are compared with those obtained at a JMA surface station as well as with those observed in the upper troposphere by the CONTRAIL project.

2. Methods

2.1 Aircraft sampling and sample analysis

Since the technical details are given by Tsuboi et al. (2013), a short description of the C-130H aircraft observation and its measurement system is provided here. The mid-tropospheric observation program is conducted by JMA in cooperation with the Japan Ministry of Defense for the aircraft operation and with the Meteorological Research Institute (MRI) for measurement techniques. The C-130H cargo aircraft flies once a month to bring supplies from Atsugi Base (35.45°N, 139.45°E), located in Kanagawa Prefecture close to Tokyo, to Minamitorishima (MNM; 24.28°N, 153.98°E), a small and isolated coral island located 1,848 km southeast of Tokyo (Fig. 1). The flight altitude is approximately 6 km, and the flight time is approximately 4 h. During the flight from Atsugi Base to MNM, air samples are collected in approximately 24 flasks, of which 17–20 are made during the level flight, and the other 4–7 samples are made during descent toward MNM (Fig. 2). Therefore, from one flight, we obtain a highly resolved horizontal profile (approx-

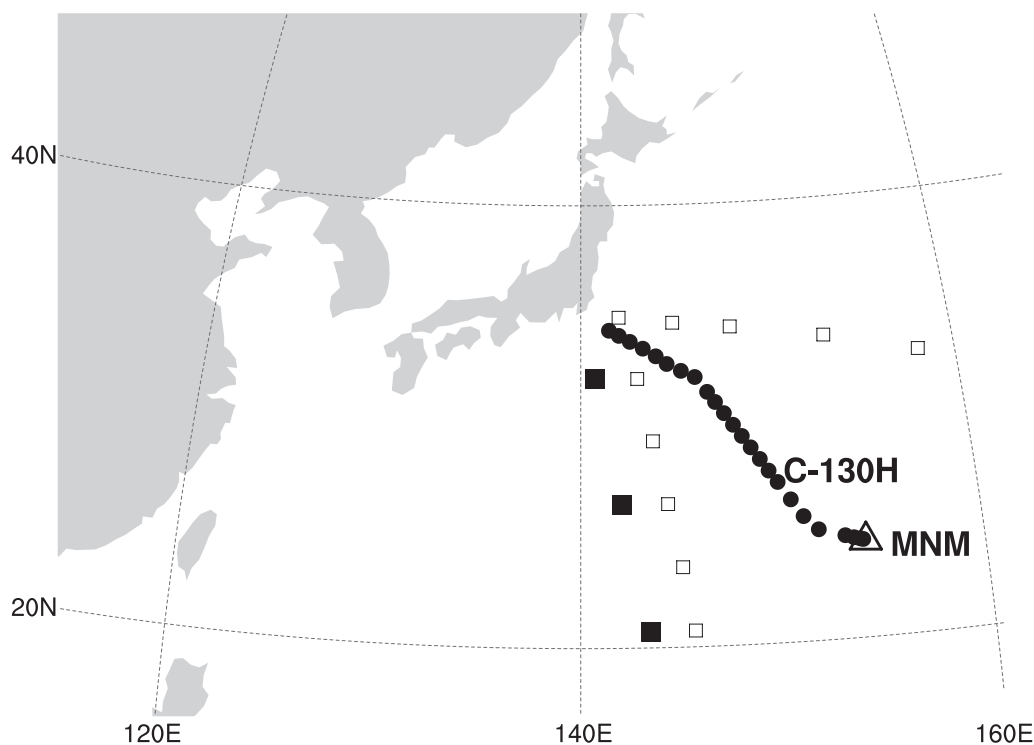


Fig. 1. Flask sampling points of the C-130H aircraft observation (closed circles) and CONTRAIL (closed squares represent for the Tokyo–Sydney line and open ones represent for the Tokyo–Guam and Tokyo–Honolulu lines). Open triangle denotes the location of Minamitorishima (MNM; 24.28°N, 153.98°E).

imately 100 km interval) in the mid-troposphere and a vertical profile of approximately 1–2 km resolution over MNM. As shown in Fig. 2, the sampling points do not have regular intervals. This is because flask sampling is manually conducted by JMA staff using a hand-driven pump because of limited space and lack of electric power supply. Routine operation started in February 2011 after an 8-month period of test flights from June 2010. In this study, we analyzed observational data from September 2010 to September 2012, a 25-month period that includes measurements from the initial 5 months of the test flights and 20 months of the operational flights.

Air samples from the operational flights were analyzed for concentrations of CO₂, CH₄, N₂O, and CO at the JMA, and those from the test flights were analyzed for CO₂, CH₄, and CO at the MRI. The JMA measurement system and its measurement uncertainties for each species have been described in detail by Tsuboi et al. (2013). The measurement system comprises laser-based instruments of a wavelength-scanned cavity ring-down spectroscopy analyzer (Picarro, G2301) for CO₂ and CH₄ (Crosson 2008), and an off-axis inte-

grated cavity output spectroscopy analyzer (Los Gatos, DLT100) for N₂O and CO (Baer et al. 2002). Using the analyzers installed in the JMA system, measuring concentrations of a same gas in different flasks has reproducibility with an overall precision of less than 0.06 ppm for CO₂, 0.68 ppb for CH₄, 0.03 ppb for N₂O, and 0.36 ppb for CO (Tsuboi et al. 2013). The MRI measurement system is composed of a nondispersive infrared gas analyzer for CO₂ and a gas chromatograph with a flame ionization detector for CH₄ and CO (Matsueda and Inoue 1996; Matsueda et al. 1998).

Concentrations measured by the JMA system are determined by the JMA standard gases that are traceable to the World Meteorological Organization (WMO) mole fraction scales at the Global Monitoring Division of National Oceanic and Atmospheric Administration/Earth System Research Laboratory (Zhao and Tans 2006; Dlugokencky et al. 2005; Novelli et al. 2003; Hall et al. 2007). The test flight data obtained by the MRI system were calculated to form a consistent dataset based on the WMO mole fraction scales (Tsuboi et al. 2013).

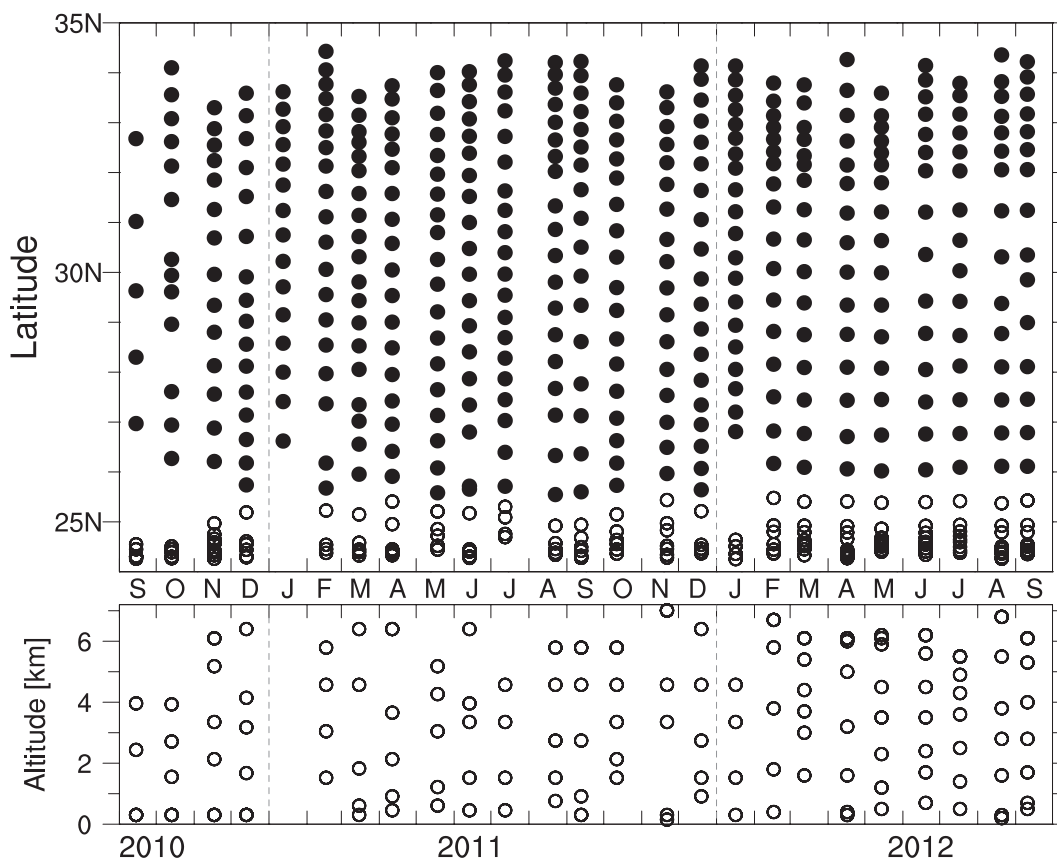


Fig. 2. Latitudinal and vertical locations of the C-130H aircraft sampling points. Sampling locations for horizontal cruising and descending sections are represented by closed and open circles respectively.

2.2 Surface and upper tropospheric data

We used the surface station data in MNM, which has been operated and maintained by JMA for approximately 20 years. For CO_2 , CH_4 , and CO , we used hourly mean data obtained from the in-situ continuous measurement (Wada et al. 2011 and references therein). For N_2O , we used data from ground-based flask air sampling, which is conducted when the C-130H arrives at MNM (Tsuboi et al. 2013). These JMA monitoring data are based on the WMO mole fraction scales, so that they can be directly compared with the C-130H measurements.

For upper tropospheric observations, we used data from CONTRAIL (<http://www.cger.nies.go.jp/contrail/>) (Machida et al. 2008). Here, we used data obtained by the automatic air sampling equipment (ASE) onboard a passenger aircraft of Japan Airlines (Matsueda and Inoue 1996; Matsueda et al. 1998, 2008). The CONTRAIL-ASE observation has been conducted on route between Japan and Australia since 1993

(Matsueda et al. 2002). The aircraft usually flies two times a month, collecting 12 air samples at an altitude of approximately 11 km between 30°S and 35°N . From April 2009 to September 2010, these data have been supplemented with measurements from other ASE flights to Guam and Honolulu. For comparison with the C-130H data, we used those data limited to a region $20\text{--}35^\circ\text{N}$ and $140\text{--}160^\circ\text{E}$ (Fig. 1). More than 1100 measurements (obtained from April 1993 to September 2012) were used to characterize a climatological feature of the data (Section 3.4). All the measurements have been calibrated by the NIES-94 and NIES-09 scales for CH_4 and CO_2 , respectively. The NIES standard scales are slightly different from those of the WMO (approximately 4 ppb for CH_4 (http://ds.data.jma.go.jp/gmd/wcc/ch4/com_annex2.html), and less than 0.1 ppm for CO_2 (Machida et al. 2011)), but those differences are negligible for our comparison with the C-130H measurements.

3. Results and discussion

3.1 Temporal variations in the mid-troposphere

Figure 3 shows temporal variations of CO₂, CO, CH₄, and N₂O observed in the mid-troposphere (at approximately 6 km) during the C-130H cruising flights between Atsugi Base and MNM. In this figure, all the measurements obtained from 25 flights (from September 2010 to September 2012) are plotted together with the MNM ground-based station data.

The CO₂ concentration in the mid-troposphere shows a distinct seasonal cycle superimposed on an increasing trend of approximately 2 ppm yr⁻¹, features similar to those observed at MNM (Fig. 3a). Moreover, large horizontal CO₂ variations (approximately 6 ppm) were observed during winter–spring. This corresponded to the period when large temporal variations were also observed at the surface. For other seasons, the horizontal CO₂ variations were mostly in the range of approximately 3 ppm. In summer, relatively low concentrations were occasionally observed with values of approximately 6–8 ppm lower than the baseline in September 2010 and July 2012. It is likely that these low values were caused by strong biosphere uptake over the Asian continent (Wada et al. 2007).

The CH₄ and CO concentrations in the mid-troposphere show similar seasonal cycles with a slight increase in winter and a decrease in summer. However, because of large variations observed during even one flight (up to approximately 120 and 150 ppb for CH₄ and CO, respectively), determination of the seasonal maximum and minimum was difficult. Such large variations were observed not only in winter–spring but also in summer. In general, high concentration values of CH₄ and CO were observed concurrently. In contrast, distinct seasonal variations of CH₄ and CO were observed at MNM. It could be attributed to increased chemical destruction by hydroxyl radical (OH) in summer, as these patterns are commonly observed at background surface monitoring sites.

The N₂O concentration observed in the mid-troposphere shows a comparable increasing trend to that observed at MNM. The observed seasonal cycles in the mid-troposphere and at MNM were not well defined, because the data records were short, and they were compounded by the large horizontal variations of approximately 1–3 ppb, which were much larger than the analytical precision (0.03 ppb). As reported by Ishijima et al. (2010), very low N₂O concentrations (approximately 300–320 ppb) were occasionally observed by CONTRAIL in the upper troposphere; they were caused by the intrusion of air from the

stratosphere where chemical loss of N₂O is significantly large. Figure 3d shows that N₂O observed in the mid-troposphere did not have such low concentrations, indicating that the air masses observed by C-130H were not influenced by the stratospheric air.

3.2 Vertical profiles over MNM

Figure 4 shows the vertical profiles of CO₂, CH₄, CO, and N₂O from the surface to approximately 7 km observed over MNM from September 2010 to September 2012. To highlight seasonal changes, the profiles in Fig. 4 were classified into four seasons, namely, December–January–February (DJF), March–April–May (MAM), June–July–August (JJA), and September–October–November (SON). Here, the concentrations of CO₂ and N₂O, both of which have increasing trends, were detrended a priori using linear trends at 5–7 km. However, CH₄ and CO concentrations were not detrended because the observed year-to-year changes in their vertical profiles were much smaller than the seasonal variations.

During DJF and MAM, the CO₂ profiles showed negative vertical gradients, that is, the concentration decreased as the altitude increased. Maximum vertical difference in MAM was approximately 5 ppm between the surface and the mid-troposphere. No significant vertical gradients were found in other seasons.

The most prominent feature of the seasonal variation in the vertical profiles was found in CH₄ and CO. During JJA, the CH₄ as well as the CO profiles showed positive gradients with height in contrast to the negative gradient of CO₂. The vertical differences between the surface and the mid-troposphere were observed to be 30–40 ppb for CH₄ as well as for CO. These CH₄ and CO positive gradients become negative during DJF, MAM, and SON, showing similar decrease with height as CO₂. For DJF, when the negative gradient was the steepest, the vertical differences were up to approximately 60 ppb and 120 ppb for CH₄ and CO, respectively. During MAM, high CO concentrations of approximately 170 ppb were often observed at the mid-altitude range from 2 to 4 km.

For the N₂O vertical profiles, there did not exist any significant vertical gradient throughout the year. Vertical variations of N₂O were mostly within a range of 2 ppb.

3.3 CO₂ seasonal cycle

Figure 5a shows time series of CO₂ concentrations observed at the MNM station. Also shown in the figure are the CO₂ values at altitudes of 2–4 and 5–7 km over MNM observed by C-130H as well as those in the

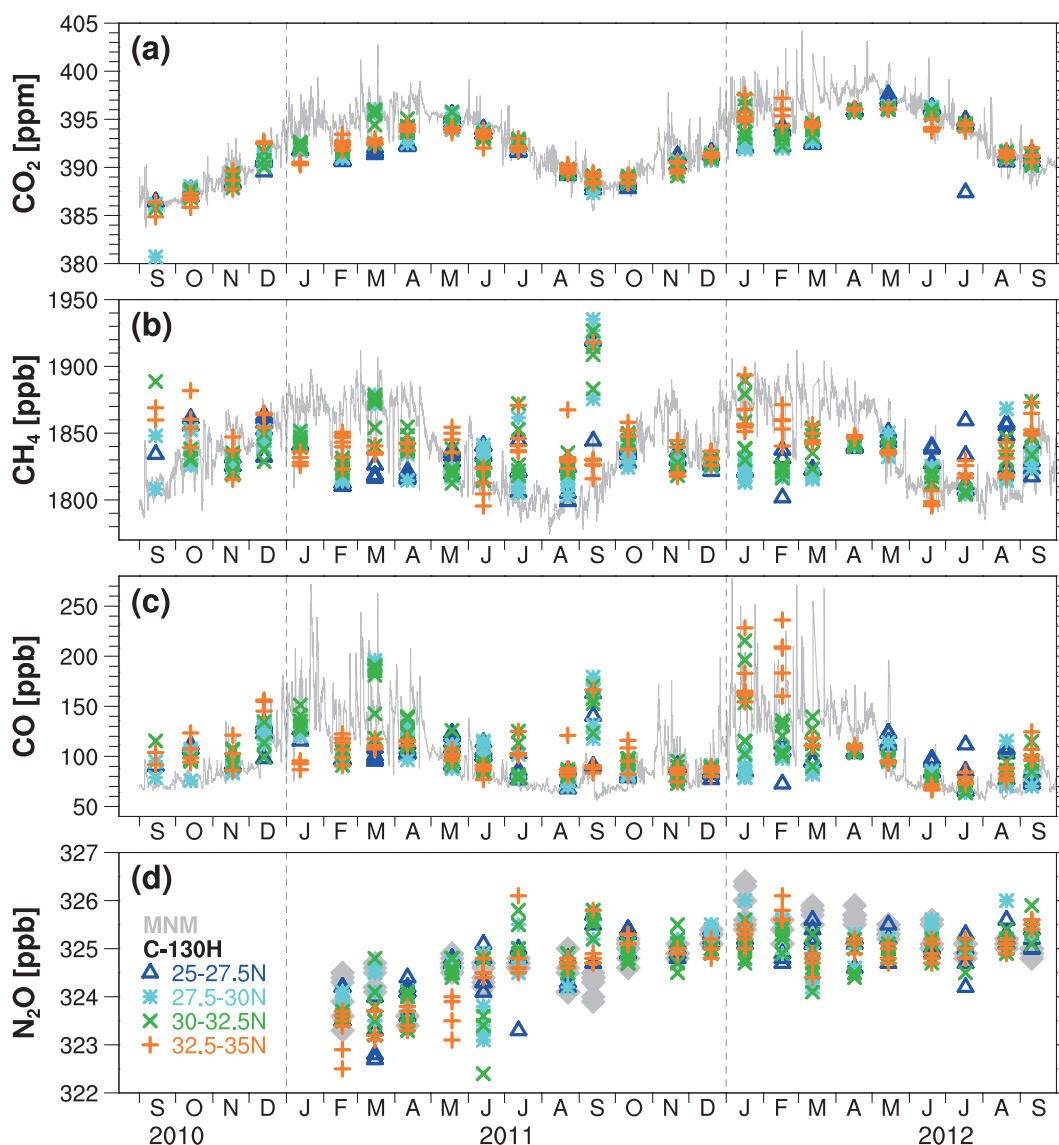


Fig. 3. Time series of observed concentrations of CO₂ (a), CH₄ (b), CO (c) and N₂O (d). Blue, cyan, green and orange symbols denote observations obtained by the level flights (5–7 km) of C-130H between Atsugi and MNM, respectively for 25–27.5°N, 27.5–30°N, 30–32.5°N and 32.5–35°N. Gray lines and diamonds respectively denote observations by continuous measurements of CO₂, CH₄ and CO and flask measurements of N₂O at the MNM ground-based station.

upper troposphere (approximately 11 km) observed by CONTRAIL in the latitude range from 20°N to 25.5°N. The concentrations were fitted with a smooth curve by the digital filtering technique of Nakazawa et al. (1997). Figure 5b shows average seasonal cycles obtained by the digital filtering with three Fourier harmonics and smoothed by the Butterworth filter, which attenuates the third-order component of the Fourier harmonics by 50%.

For the average seasonal cycles shown in Fig. 5b, CO₂ concentrations in the mid-troposphere have a seasonal maximum in May and a minimum in September, similar to those observed at MNM and in the upper troposphere. The seasonal amplitude in the mid-troposphere is approximately 6–7 ppm, slightly smaller than that at MNM. Between the mid- and upper-troposphere, there exists almost no difference in the seasonal cycle (in magnitude and phase). In contrast, using monthly

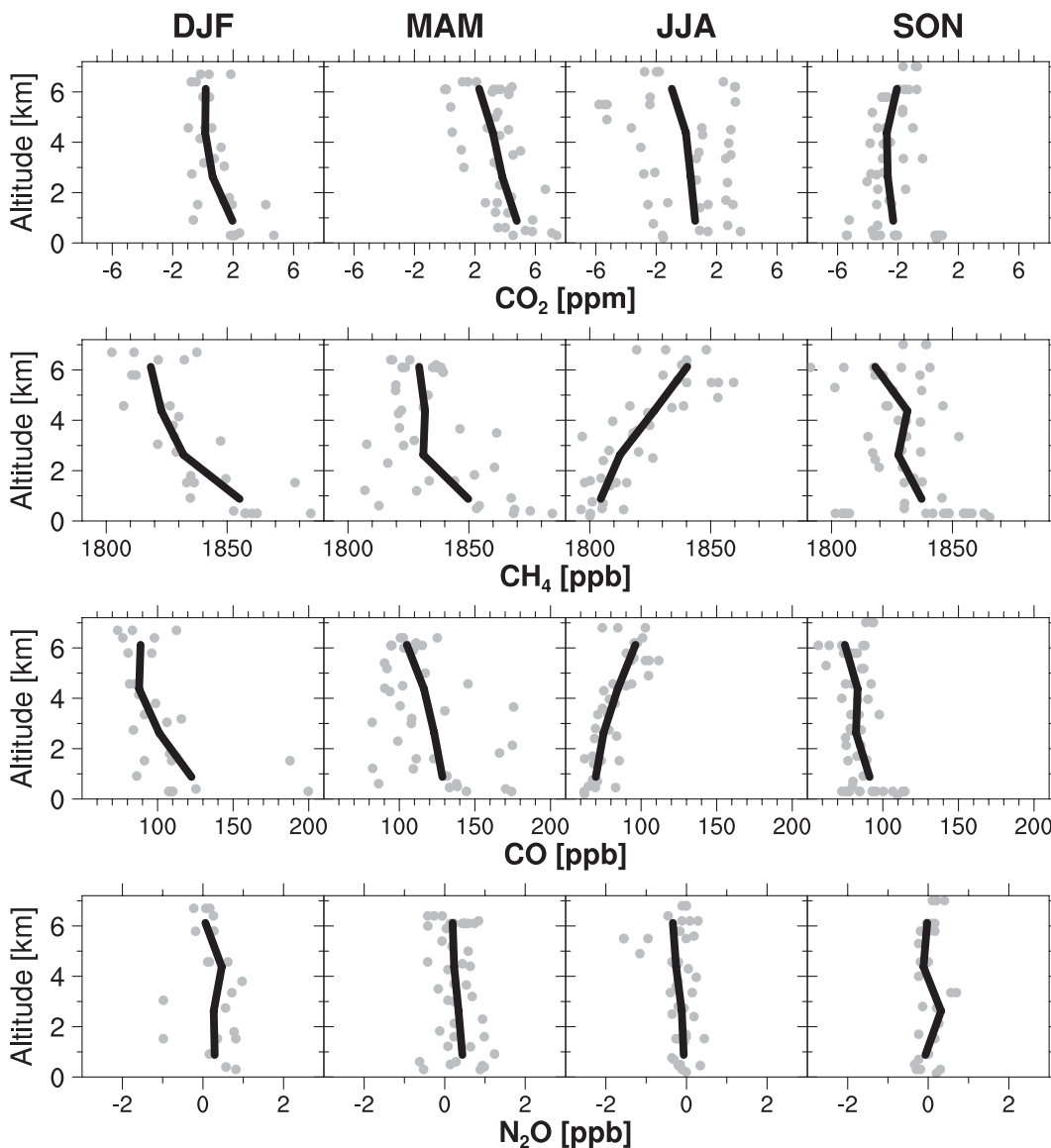


Fig. 4. Vertical profiles of observed concentrations, obtained over MNM (in the latitudinal range of 24–25.5°N), for CO₂ (top panels), CH₄ (upper-middle panels), CO (lower-middle panels) and N₂O (bottom panels). Gray circles represent individual observations and black solid line represents averaged vertical profile for each season: December–January–February (DJF), March–April–May (MAM), June–July–August (JJA) and September–October–November (SON). Concentrations of CO₂ and N₂O were detrended using the linear trends at 5–7 km.

vertical aircraft measurements over the northeastern coast of Japan (50 km off the coast of Sendai), just off the Asian continent, Nakazawa et al. (1993) showed that the CO₂ seasonal amplitude in the upper portion of the free troposphere was approximately 3 ppm lower and lagged by approximately 1 month compared to the seasonal cycle observed in the boundary layer. This suggests that there is a significant vertical mixing

before air reaches MNM.

3.4 High CH₄ concentrations in the mid-troposphere

High concentration events of CH₄ in the mid-troposphere were found, as shown in Fig. 3. In this section, we present some results from our analysis of these high CH₄ concentration events, as well as of CO and CO₂, and compare them to the CONTRAIL and MNM

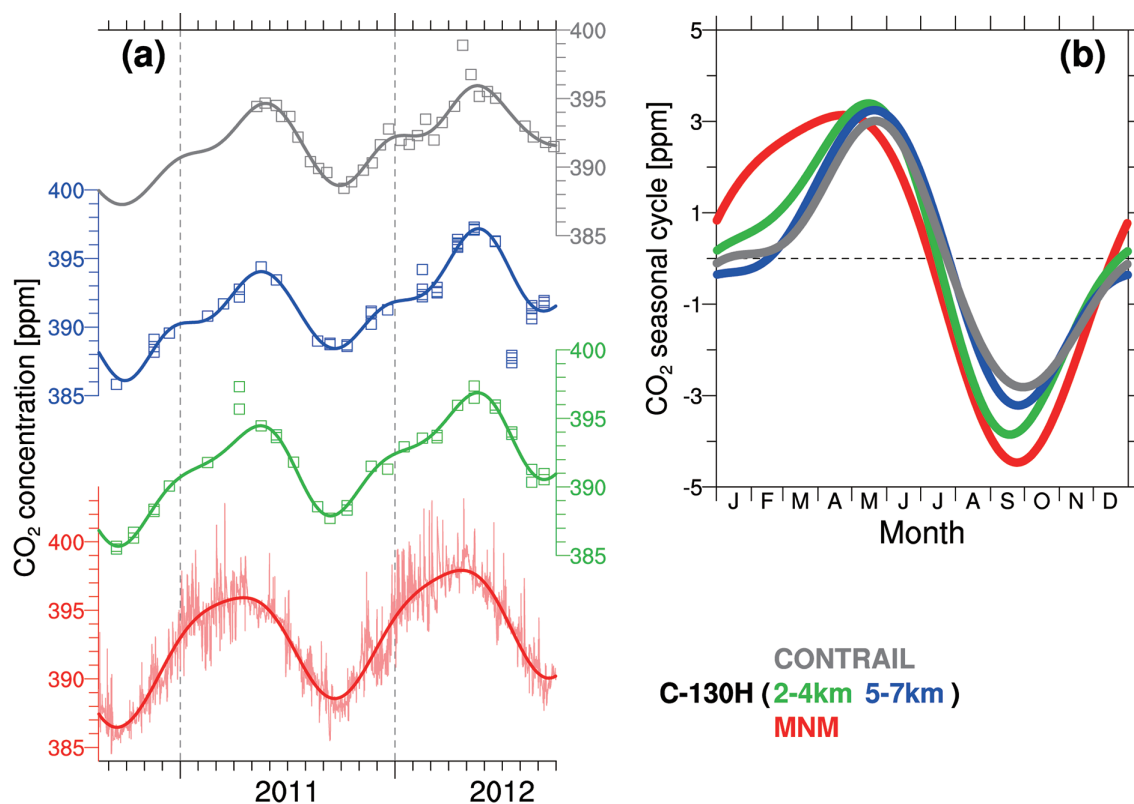


Fig. 5. Time series of CO₂ concentrations at MNM (red), 2–4 km (green) and 5–7 km (blue) from C-130H, and in the upper-troposphere from CONTRAIL (gray), with their best fit curves (a) and their average seasonal cycles calculated by the digital curve fitting method (b). The measurements by C-130H and CONTRAIL are spatially limited to the latitude range of 20–25.5°N.

observations.

Figure 6 shows seasonal variations of CH₄ and CO concentrations observed during the level flights of C-130H (5–7 km), along with those observed at MNM and by CONTRAIL. In the figure, the MNM and CONTRAIL data are depicted as monthly normalized frequencies derived from the two-decade-long data (April 1993–September 2012). The CONTRAIL data are spatially limited to the latitude zone 20°N–35°N. For comparison with the C-130H measurements obtained mainly during 2011, the CH₄ concentration values from MNM and CONTRAIL were normalized to the reference year of 2011 (CH₄²⁰¹¹) as follows.

$$\text{CH}_4^{2011}(t - \text{int}(t) + 2011) = \text{CH}_4(t) - \text{CH}_4^{\text{trend}}(t) + \text{CH}_4^{\text{trend}}(t - \text{int}(t) + 2011), \quad (1)$$

where CH₄(*t*) and CH₄^{trend}(*t*) are the measured CH₄ concentration and its long-term trend, respectively, at time *t* (expressed as fractional year). This procedure was employed because atmospheric concentrations

have significantly large long-term variations (Dlugokencky et al. 2009). The long-term trend component CH₄^{trend} was derived by the same method used by Terao et al. (2011). The method employs the digital filtering technique of Nakazawa et al. (1997), and the long-term trend is obtained from a 36-month low-pass filter. For the CH₄ measurements by C-130H, we did not perform such correction because the measurement period was relatively short.

Figures 6a and 6c show that high CH₄ concentrations appear specifically during winter–spring and summer–fall in the mid-troposphere. In the next two subsections, we discuss these high CH₄ concentrations.

a. Winter–spring

From winter to spring (December–March), high-concentration events were observed in the mid-troposphere for CH₄ as well as for CO at the same time. Higher end values for each flight were observed to be approximately 1870 ppb and 180 ppb for CH₄ and CO, respec-

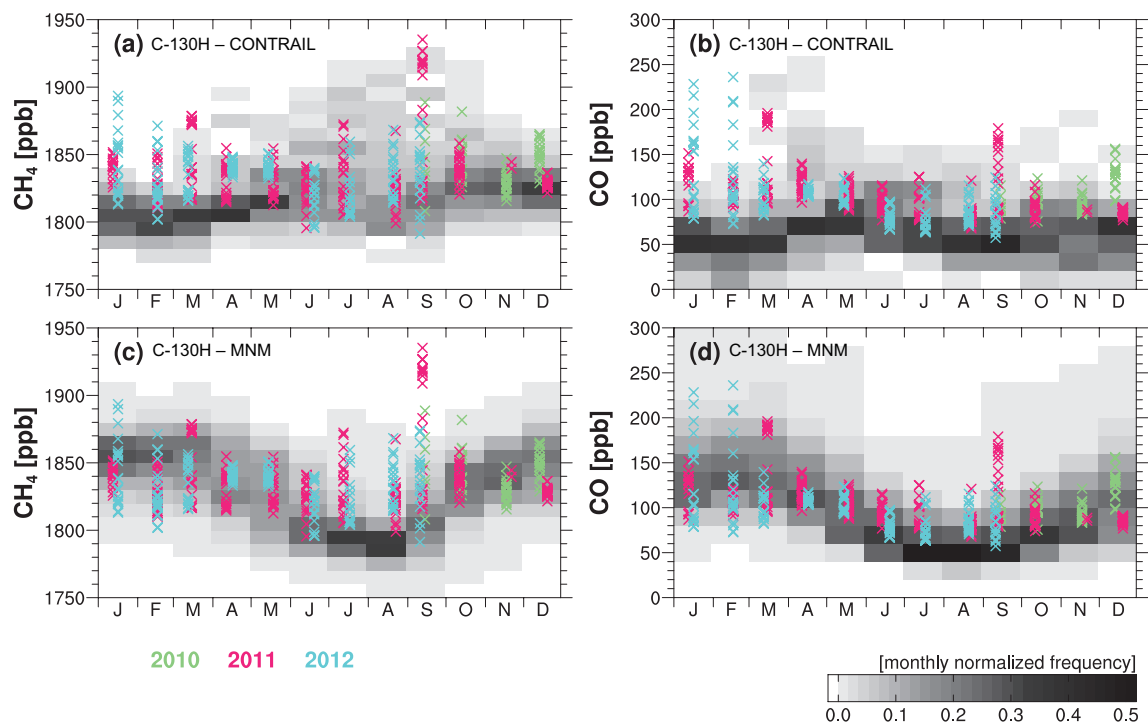


Fig. 6. Monthly normalized frequencies of CH₄ (left panels) and CO (right panels) concentrations from the observations at MNM (bottom panels) and from CONTRAIL (upper panels) superimposed on the C-130H measurements (crosses). The CH₄ concentrations from MNM and CONTRAIL are modified to the reference year of 2011 (see the main text for detail). The normalized frequency is derived from the number of measurements in each fixed bin (the intervals are 10 and 20 ppb for CH₄ and CO respectively) divided by the total number of measurements for each month.

tively, and are nearly comparable to those observed at the MNM surface station (Figs. 6c and 6d). At MNM, 32% and 22% of the data measured during the winter–spring period of 1993–2012 were larger than 1870 ppb and 180 ppb for CH₄ and CO, respectively. (Note that the CH₄ data were normalized for 2011) Conversely, CONTRAIL rarely observed high-concentration events in the upper troposphere during January–February though it is observed that some high CH₄ and CO events start to appear at the beginning of March (Figs. 6a and 6b). These low occurrences of the high-concentration event in the upper troposphere during winter were probably because of the fact that a strong atmospheric stratification suppressed vertical transport to the upper troposphere.

Simultaneously, high concentrations of CH₄ and CO were observed in the mid-troposphere. For instance, Fig. 7a shows horizontal concentration profiles of CH₄ and CO observed on 16 January 2012. During this flight, a CH₄ concentration peak was observed with concomitant CO and CO₂ peaks. The concomitant high

CO and CO₂ suggest that the observed high CH₄ air masses originated from China, where there are a large amount of combustion sources (i.e., fossil fuel use and burning of biomass/biofuels). These high concentrations of GHGs and CO in the mid-troposphere were probably the result of updraft of polluted air from the boundary layer to the free-troposphere over China, followed by a fast westerly advective transport. Such a transport mechanism of Asian outflow was reported by Oshima et al. (2012) during campaign-style aircraft measurements of CO and black carbon. This transport feature is typical for winter and is important for long-range transport of Asian polluted air, which occasionally reaches even the western regions of North America (Liang et al. 2004).

Figures 8a and 8b show concentration relationships of CO–CH₄ and CO₂–CO, respectively, observed in the mid-troposphere. For December–March, the average enhancement ratio of CH₄/CO (the slope of the regression line; $\Delta\text{CH}_4/\Delta\text{CO}$) observed was 0.47 ppb/ppb (Fig. 8a). This number is comparable to those

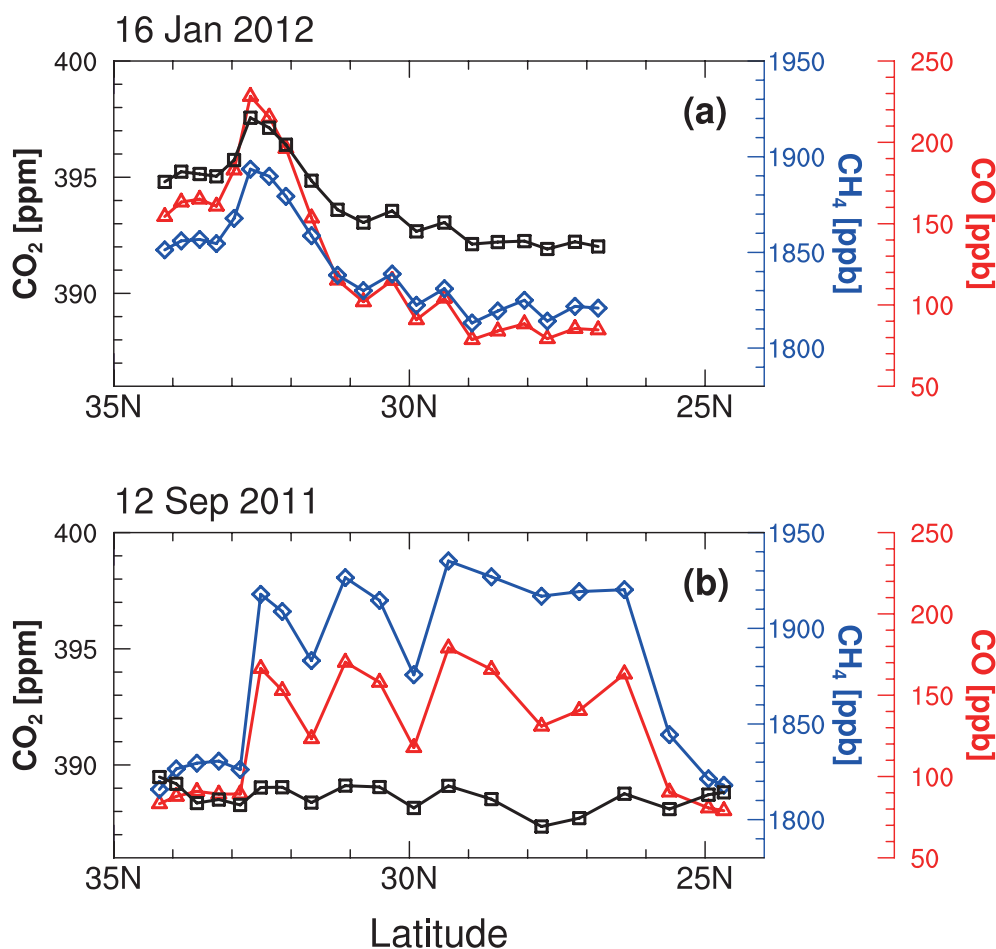


Fig. 7. Latitudinal profiles of CO₂ (black), CH₄ (blue), and CO (red) observed by the C-130H aircraft on 16 January 2012 (a) and 12 September 2011 (b).

obtained by other aircraft measurements in the mid- and upper-troposphere over the western North Pacific and at MNM. Based on the campaign-style aircraft measurements of the Transport and Chemical Evolution Over the Pacific (TRACE-P) program, Xiao et al. (2004) reported $\Delta\text{CH}_4/\Delta\text{CO}$ values of 0.38–0.65 ppb/ppb. From the passenger aircraft measurements of the Civil Aircraft for the Regular Investigation of the atmosphere Based on an Instrument Container (CARIBIC) program in the upper troposphere between South China and Philippines during April, Lai et al. (2010) reported ratios of 0.3–0.8 ppb/ppb. In addition, Wada et al. (2011) reported ratios of approximately 0.5–0.8 ppb/ppb for the same season using the MNM measurements. Thus, values of the $\Delta\text{CH}_4/\Delta\text{CO}$ ratio appear to be height independent over the western North Pacific. However, it should be noted that the frequency of

high-concentration events are quite different between the mid- and upper-tropospheric regions. For the enhancement ratio of CO/CO_2 ($\Delta\text{CO}/\Delta\text{CO}_2$), the C-130H aircraft observed 16.2 ppb/ppm on average (Fig. 8b). This number is slightly smaller than the range reported by TRACE-P (20–33 ppb/ppm; Suntharalingam et al. 2004), CARIBIC (15.6–29.3 ppb/ppm; Lai et al. 2010), and at MNM (approximately 30 ppb/ppm; Wada et al. 2011).

The ratios of $\Delta\text{CH}_4/\Delta\text{CO}$ and $\Delta\text{CO}/\Delta\text{CO}_2$ observed in the mid-troposphere were much larger than those produced by biomass burning (both numbers were generally less than 0.1 in our study) (Andreae and Merlet 2001). Therefore, for winter–spring, it is probable that the observed high concentrations of CH₄, as well as of CO and CO₂, were caused mostly by industrial fossil fuel burning. Similar implications have been

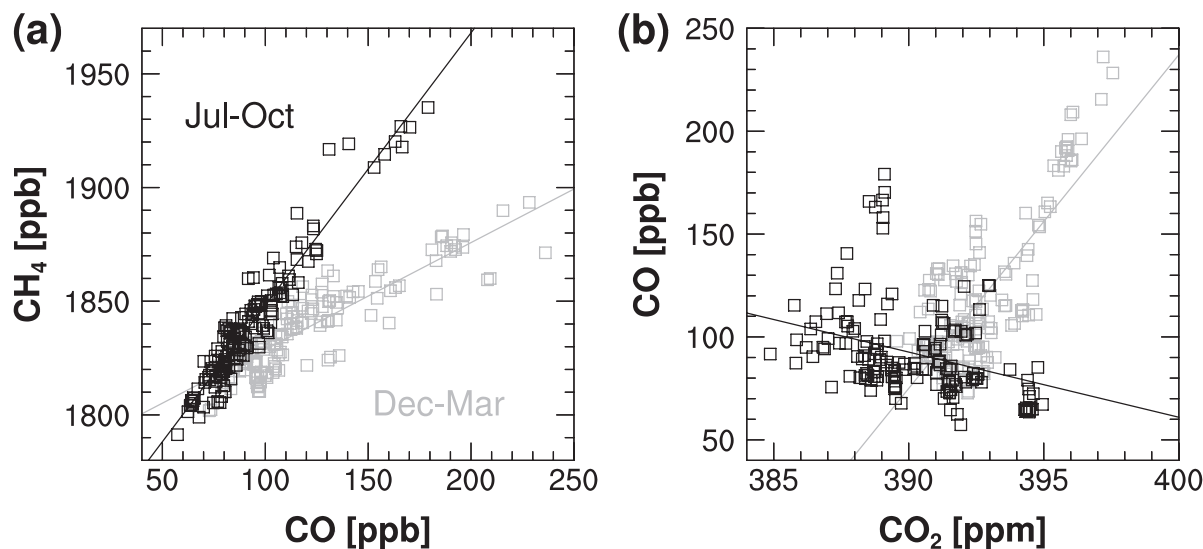


Fig. 8. Correlation plots for CO–CH₄ (a) and CO₂–CO (b) observed by the C-130H flights for July–October (black) and for December–March (gray). Solid lines denote the regression lines.

identified by the observations of TRACE-P, CARIBIC, and MNM.

b. Summer–fall

Although previous campaign-style aircraft measurements focused on high concentrations of GHGs and CO during winter–spring, we have also found notably high CH₄ concentrations in the mid-troposphere during summer–fall (July–October), as shown in Figs. 6a and 6c. A CH₄ concentration value, as large as 1935 ppb, was observed on 12 September 2011. The C-130H flights in other years also observed CH₄ concentrations higher than 1860 ppb for this season. These high concentrations observed in the mid-troposphere were above the seasonal baseline values in the upper troposphere and at the surface observed by CONTRAIL and the MNM station, respectively. (The seasonal baseline values are derived from most frequently observed values, i.e., darker shaded areas in Figs. 6a and 6c) These features are consistent with the positive vertical gradients of CH₄ over MNM, as shown in Fig. 4. Approximately 24% of the upper troposphere CH₄ data obtained by CONTRAIL for July–October were larger than 1860 ppb (note again the data corrected for 2011). However, at the surface, only 4% of the data from MNM were larger than 1860 ppb. Also during this period, high concentrations of CO were observed in the mid-troposphere, and they were higher than the seasonal baseline values in the upper troposphere and at the surface (Figs. 6b and 6d).

Figure 7b shows horizontal concentration profiles observed on 12 September 2011. During this flight, CH₄ variation with extremely high concentrations correlated well with that of CO. Thus, during July–October, an average $\Delta\text{CH}_4/\Delta\text{CO}$ is 1.2 ppb/ppb notably larger than 0.47 ppb/ppb observed during winter–spring (Fig. 8a). In contrast to the winter–spring flights, however, the September flight did not observe any high CO₂ concentrations. This was probably because of the balancing of fossil fuel emitted CO₂ and the terrestrial biospheric net uptake.

The significant correlation of CH₄ with CO in the mid-troposphere indicates that the observed air masses originated from combustion sources in Asia, as was the case during winter–spring. However, compared to CO, larger values of CH₄ were observed in summer–fall than in winter–spring, resulting in higher $\Delta\text{CH}_4/\Delta\text{CO}$ ratios as indicated in the previous paragraph. These higher CH₄ contributions probably came from an increase in biogenic emissions during summer. However, the seasonal variation in the OH concentration could also contribute to the observed seasonal changes in $\Delta\text{CH}_4/\Delta\text{CO}$ with the greatest OH destruction occurring in the summer. However, Wada et al. (2011) inferred that the OH destruction contribution to the observed $\Delta\text{CH}_4/\Delta\text{CO}$ ratio at MNM is less than 15% during the summer. This leads us to conclude that the larger $\Delta\text{CH}_4/\Delta\text{CO}$ in summer–fall than in winter–spring observed by C-130H is mostly attributable to increased CH₄ emissions.

Figure 6a shows that the CONTRAIL aircraft measurements in the upper troposphere also showed similar high CH₄ concentrations during the same seasonal period. Using CH₄ isotopic ratios, Umezawa et al. (2012) suggested that the high CH₄ concentration in the upper troposphere contained significant contribution from the biogenic sources (e.g., rice paddies and livestock) in Asia. Moreover, from the CARIBIC measurements, Schuck et al. (2010) and Baker et al. (2012) also found high CH₄ concentrations in the upper troposphere over South Asia during the Indian summer monsoon season. Baker et al. (2012) suggested a significant contribution of biogenic sources to the observed high CH₄ by calculating relationships with concomitantly observed ethane (C₂H₆) and CO concentrations.

These high CH₄ concentrations over South Asia observed by CARIBIC are probably transported to the western North Pacific region where they are subsequently observed by C-130H and CONTRAIL. In fact, Umezawa et al. (2012) performed a regionally-tagged CH₄ transport simulation and found that the main contributing source region to the high CH₄ they observed is South Asia with East Asia being the second most important. Moreover, Niwa et al. (2012) demonstrated that the active summer convection over South Asia causes a significant uplifting of surface flux signals to the upper troposphere. Over South Asia, Baker et al. (2012) observed a $\Delta\text{CH}_4/\Delta\text{CO}$ ratio of 1.9–4.4 ppb/ppb for July–September. Therefore, the ratio of 1.2 ppb/ppb, we observed in the mid-troposphere, suggests that the strong biogenic CH₄ signal from South Asia was slightly diluted by signals from combustion sources in East Asia before reaching the western North Pacific. This should be further verified by forward and inverse model simulations, but left as a future work.

At the inland monitoring station of Waliguan in China, summer high CH₄ concentrations are also being observed (Zhou et al. 2004). This fact gives additional support to claim that the aircraft measurements in the mid- and upper-troposphere over the western North Pacific are able to capture CH₄ emission signals from the Asian continent. In contrast, the surface MNM station does not observe such high CH₄ concentrations during summer probably because Pacific anticyclones prevent any strong atmospheric transport from the Asian continent to MNM during this season. Therefore, to capture CH₄ emission signals from the continent, measurements in the mid- and upper-troposphere are indispensable.

4. Conclusions

Using the C-130H aircraft observation operated by JMA, we characterized the seasonal variations of GHGs and CO in the mid-troposphere over the western North Pacific. The C-130H observations showed increasing trends of CO₂ and N₂O concentrations in the mid-troposphere. These observations also showed large variability in CH₄ and CO through the year. The result of not observing low N₂O concentration indicated that the air masses observed by C-130H were not influenced by the stratospheric air. From vertical profile observations over MNM, we found higher concentrations of CH₄ and CO at higher altitude during summer. For CO₂, the timing of seasonal maximum and minimum was shown to be height independent from the surface to the upper troposphere.

A notable finding from the C-130H aircraft observation was the high CH₄ concentration events in the mid-troposphere during summer–fall. The C-130H observed high CH₄ concentrations concomitantly with high CO concentrations for winter–spring as well as for summer–fall. For the high concentration events observed during winter–spring, an average ratio $\Delta\text{CH}_4/\Delta\text{CO}$ of 0.47 ppb/ppb is consistent with those observed by previous studies and is suggestive of the air masses originating from industrial fossil fuel combustion. For the high concentration events during summer–fall, the average ratio $\Delta\text{CH}_4/\Delta\text{CO}$ increased to 1.2 ppb/ppb, which is attributable to increased biogenic sources of CH₄ during this period. Comparing with the results of the previous studies, air masses observed by C-130H during summer–fall might be a mixture of air masses from East and South Asia. It should be noted that the surface station rarely observes such high CH₄ concentrations during this season giving added value to the mid-tropospheric C-130H measurements in reducing uncertainties in the CH₄ emission estimates.

Using transport models with the C-130H measurements will greatly improve our understanding of the Asian outflow of GHGs and CO over the western North Pacific. Furthermore, by combining the mid-tropospheric C-130H measurements with those by the surface MNM station and by CONTRAIL in the upper troposphere, they would constitute a good reference data set for validating satellite CO₂ and CH₄ data retrieved from thermal infrared spectra that have concentration information mainly from the mid- to upper-troposphere (Chahine et al. 2008; Saitoh et al. 2009, 2012; Crevoisier et al. 2009, 2013; Kulawik et al. 2013).

The dataset of the GHGs and CO concentrations

obtained by C-130H are available on the WMO World Data Centre for Greenhouse Gases (<http://ds.data.jma.go.jp/gmd/wdcgg/wdcgg.html>). Continuation of this aircraft measurement program for many years would promote our understanding of the spatial variations of the GHG fluxes in Asia and of those long-term variations induced by the rapidly growing human activities and climate change.

Acknowledgments

We would like to acknowledge the staff of the Japan Ministry of Defense for supporting the C-130H aircraft observation. We are also thankful to Keiichi Katsumata and Hisayo Sandanbata of NIES for their technical measurement support on the CONTRAIL flask sampling. We would like to extend our sincere appreciation to Takakiyo Nakazawa of Tohoku University for providing us the digital filtering program. We also thank Kaz Higuchi of York University for his comments on the manuscript. Comments from two anonymous reviewers helped to improve the manuscript. They were greatly appreciated.

References

- Baer, D. S., J. B. Paul, M. Gupta, and A. O'Keefe, 2002: Sensitive absorption measurements in the near-infrared region using off-axis integrated-cavity-output spectroscopy. *Appl. Phys. B*, **75**, 261–265.
- Baker, A. K., T. J. Schuck, C. A. M. Brenninkmeijer, A. Rauthe-Schöch, F. Slemr, P. F. J. van Velthoven, and J. Lelieveld, 2012: Estimating the contribution of monsoon-related biogenic production to methane emissions from South Asia using CARIBIC observations. *Geophys. Res. Lett.*, **39**, L10813, doi:10.1029/2012GL051756.
- Chahine, M. T., L. Chen, P. Dimotakis, X. Jiang, Q. Li, E. T. Olsen, T. Pagano, J. Randerson, and Y. L. Yung, 2008: Satellite remote sounding of mid-tropospheric CO₂. *Geophys. Res. Lett.*, **35**, L17807, doi:10.1029/2008GL035022.
- Crevoisier, C., D. Nobileau, R. Armante, L. Crépeau, T. Machida, Y. Sawa, H. Matsueda, T. Schuck, T. Thonat, J. Pernin, N. A. Scott, and A. Chédin, 2013: The 2007–2011 evolution of tropical methane in the mid-troposphere as seen from space by MetOp-A/IASI. *Atmos. Chem. Phys.*, **13**, 4279–4289.
- Crevoisier, C., A. Chédin, H. Matsueda, T. Machida, R. Armante, and N.A. Scott, 2009: First year of upper tropospheric integrated content of CO₂ from IASI hyperspectral infrared observations. *Atmos. Chem. Phys.*, **9**, 4797–4810.
- Dlugokencky, E. J., L. Bruhwiler, J. W. C. White, L. K. Emmons, P. C. Novelli, S. A. Montzka, K. A. Masarie, P. M. Lang, A. M. Crotwell, J. B. Miller, and L. V. Gatti, 2009: Observational constraints on recent increases in the atmospheric CH₄ burden. *Geophys. Res. Lett.*, **36**, L18803, doi:10.1029/2009GL039780.
- Dlugokencky, E. J., R. C. Myers, P. M. Lang, K. A. Masarie, A. M. Crotwell, K. W. Thoning, B. D. Hall, J. W. Elkins, and L. P. Steele, 2005: Conversion of NOAA atmospheric dry air CH₄ mole fractions to a gravimetrically prepared standard scale. *J. Geophys. Res.*, **110**, D18306, doi:10.1029/2005JD006035.
- Gregg, J. S., R. J. Andres, and G. Marland, 2008: China: Emissions pattern of the world leader in CO₂ emissions from fossil fuel consumption and cement production. *Geophys. Res. Lett.*, **35**, L08806, doi:10.1029/2007GL032887.
- Gurney, K., R. Law, A. Denning, and TransCom 3 modelers, 2002: Towards robust estimates of CO₂ sources and sinks using atmospheric transport models. *Nature*, **415**, 626–630.
- Hall, B. D., G. S. Dutton, and J. W. Elkins, 2007: The NOAA nitrous oxide standard scale for atmospheric observations. *J. Geophys. Res.*, **112**, D09305, doi:10.1029/2006JD007954.
- Huang, J., A. Golombek, R. Prinn, R. W. P. Fraser, P. Simmonds, E. J. Dlugokencky, B. Hall, J. Elkins, P. Steele, R. Langenfelds, P. Krummel, G. Dutton, and L. Porter, 2008: Estimation of regional emissions of nitrous oxide from 1997 to 2005 using multinet network measurements, a chemical transport model, and an inverse method. *J. Geophys. Res.*, **113**, D17313, doi:10.1029/2007JD009381.
- Ishijima, K., P. K. Patra, M. Takigawa, T. Machida, H. Matsueda, Y. Sawa, L. P. Steele, P. B. Krummel, R. L. Langenfelds, S. Aoki, and T. Nakazawa, 2010: Stratospheric influence on the seasonal cycle of nitrous oxide in the troposphere as deduced from aircraft observations and model simulations. *J. Geophys. Res.*, **115**, D20308, doi:10.1029/2009JD013322.
- Ito, A., and M. Inatomi, 2012: Use of a process-based model for assessing the methane budgets of global terrestrial ecosystems and evaluation of uncertainty. *Biogeosciences*, **9**, 759–773.
- Jacob, D. J., J. H. Crawford, M. M. Kleb, V. S. Connors, R. J. Bendura, J. L. Raper, G. W. Sachse, J. C. Gille, L. Emmons, and C. L. Heald, 2003: Transport and Chemical Evolution over the Pacific (TRACE-P) aircraft mission: Design, execution, and first results. *J. Geophys. Res.*, **108**, 9000, doi:10.1029/2002JD003276.
- Kulawik, S. S., J. R. Worden, S. C. Wofsy, S. C. Biraud, R. Nassar, D. B. A. Jones, E. T. Olsen, R. Jimenez, S. Park, G. W. Santoni, B. C. Daube, J. V. Pittman, B. B. Stephens, E. A. Kort, G. B. Osterman, and TES team, 2013: Comparison of improved Aura Tropospheric Emission Spectrometer CO₂ with HIPPO and SGP aircraft profile measurements. *Atmos. Chem. Phys.*, **13**, 3205–3225.
- Lai, S. C., A. K. Baker, T. J. Schuck, P. van Velthoven, D. E.

- Oram, A. Zahn, M. Hermann, A. Weigelt, F. Slemr, C. A. M. Brenninkmeijer, and H. Ziereis, 2010: Pollution events observed during CARIBIC flights in the upper troposphere between South China and the Philippines. *Atoms. Chem. Phys.*, **10**, 1649–1660.
- Liang, Q., L. Jaeglé, D. A. Jaffe, P. Weiss-Penzias, A. Heckman, and J. A. Snow, 2004: Long-range transport of Asian pollution to the northeast Pacific: Seasonal variations and transport pathways of carbon monoxide. *J. Geophys. Res.*, **109**, D23S07, doi:10.1029/2003JD004402.
- Machida, T., K. Kita, Y. Kondo, D. Blake, S. Kawakami, G. Inoue, and T. Ogawa, 2002: Vertical and meridional distributions of the atmospheric CO₂ mixing ratio between northern midlatitudes and southern subtropics. *J. Geophys. Res.*, **107**, 8401, doi:10.1029/2001JD000910.
- Machida, T., H. Matsueda, Y. Sawa, Y. Nakagawa, K. Hiro-tani, N. Kondo, K. Goto, T. Nakazawa, K. Ishikawa, and T. Ogawa, 2008: Worldwide measurements of atmospheric CO₂ and other trace gas species using commercial airlines. *J. Atmos. Oceanic Technol.*, **25**, 1744–1754.
- Machida, T., Y. Tohjima, K. Katsumata, and H. Mukai, 2011: A new CO₂ calibration scale based on gravimetric one-step dilution cylinders in National Institute for Environmental Studies–NIES 09 CO₂ scale. *15th WMO/IAEA Meeting of Experts on Carbon Dioxide, Other Greenhouse Gases and Related Tracers Measurements Techniques* (WMO/TD-No. 1553), WMO/GAW Report, **194**, 165–169.
- Matsueda, H., and H. Y. Inoue, 1996: Measurements of atmospheric CO₂ and CH₄ using a commercial airliner from 1993 to 1994. *Atmos. Environ.*, **30**, 1647–1655.
- Matsueda, H., H. Y. Inoue, and M. Ishii, 2002: Aircraft observation of carbon dioxide at 8–13 km altitude over the western Pacific from 1993 to 1999. *Tellus B*, **54**, 1–21.
- Matsueda, H., H. Y. Inoue, Y. Sawa, Y. Tsutsumi, and M. Ishii, 1998: Carbon monoxide in the upper troposphere over the western Pacific between 1993 and 1996. *J. Geophys. Res.*, **103**, 19093–19110.
- Matsueda, H., T. Machida, Y. Sawa, Y. Nakagawa, K. Hiro-tani, H. Ikeda, N. Kondo, and K. Goto, 2008: Evaluation of atmospheric CO₂ measurements from new flask air sampling of JAL airliner observations. *Pap. Meteor. Geophys.*, **59**, 1–17.
- Nakazawa, T., M. Ishizawa, K. Higuchi, and N. B. A. Trivett, 1997: Two curve fitting methods applied to CO₂ flask data. *Environmetrics*, **8**, 197–218.
- Nakazawa, T., K. Miyashita, S. Aoki, and M. Tanaka, 1991: Temporal and spatial variations of upper tropospheric and lower stratospheric carbon dioxide. *Tellus B*, **43**, 106–117.
- Nakazawa, T., S. Morimoto, S. Aoki, and M. Tanaka, 1993: Time and space variations of the carbon isotopic ratio of tropospheric carbon dioxide over Japan. *Tellus B*, **45**, 258–274.
- Nara, H., H. Tanimoto, Y. Nojiri, H. Mukai, J. Zeng, Y. Tohjima, and T. Machida, 2011: CO emissions from biomass burning in Southeast Asia in the 2006 El Niño year: shipboard and AIRS satellite observations. *Environ. Chem.*, **8**, 213–223.
- Niwa, Y., T. Machida, Y. Sawa, H. Matsueda, T. J. Schuck, C. A. M. Brenninkmeijer, R. Imasu, and M. Satoh, 2012: Imposing strong constraints on tropical terrestrial CO₂ fluxes using passenger aircraft based measurements. *J. Geophys. Res.*, **117**, D11303, doi:10.1029/2012JD017474.
- Niwa, Y., P. K. Patra, Y. Sawa, T. Machida, H. Matsueda, D. Belikov, T. Maki, M. Ikegami, R. Imasu, S. Maksyutov, T. Oda, M. Satoh, and M. Takigawa, 2011: Three-dimensional variations of atmospheric CO₂: aircraft measurements and multi-transport model simulations. *Atoms. Chem. Phys.*, **11**, 13359–13375.
- Novelli, P. C., K. A. Masarie, P. M. Lang, B. D. Hall, R. C. Myers, and J. W. Elkins, 2003: Reanalysis of tropospheric CO trends: Effects of the 1997–1998 wildfires. *J. Geophys. Res.*, **108**, 4464, doi:10.1029/2002JD003031.
- Ohara, T., H. Akimoto, J. Kurokawa, N. Horii, K. Yamaji, X. Yan, and T. Hayasaka, 2007: An Asian emission inventory of anthropogenic emission sources for the period 1980–2020. *Atmos. Chem. Phys.*, **7**, 4419–4444.
- Oshima, N., Y. Kondo, N. Moteki, N. Takegawa, M. Koike, K. Kita, H. Matsui, M. Kajino, H. Nakamura, J. S. Jung, and Y. J. Kim, 2012: Wet removal of black carbon in Asian outflow: Aerosol Radiative Forcing in East Asia (A-FORCE) aircraft campaign. *J. Geophys. Res.*, **117**, D03204, doi:10.1029/2011JD016552.
- Patra, P. K., M. Ishizawa, S. Maksyutov, T. Nakazawa, and G. Inoue, 2005: Role of biomass burning and climate anomalies for land-atmosphere carbon fluxes based on inverse modeling of atmospheric CO₂. *Global Biogeochem. Cycles*, **19**, GB3005, doi:10.1029/2004GB002258.
- Patra, P. K., Y. Niwa, T. J. Schuck, C. A. M. Brenninkmeijer, T. Machida, H. Matsueda, and Y. Sawa, 2011: Carbon balance of South Asia constrained by passenger aircraft CO₂ measurements. *Atoms. Chem. Phys.*, **11**, 4163–4175.
- Peters, G. P., G. Marland, C. L. Quéré, T. Boden, J. G. Canadell, and M. R. Raupach, 2012: Rapid growth in CO₂ emissions after the 2008–2009 global financial crisis. *Nat. Clim. Change*, **2**, 2–4.
- Saitoh, N., R. Imasu, Y. Ota, and Y. Niwa, 2009: CO₂ retrieval algorithm for the thermal infrared spectra of the Greenhouse Gases Observing Satellite: Potential of retrieving CO₂ vertical profile from high-resolution FTS sensor. *J. Geophys. Res.*, **114**, D17305, doi:10.1029/2008JD011500.
- Saitoh, N., M. Touno, S. Hayashida, R. Imasu, K. Shiomi, T. Yokota, Y. Yoshida, T. Machida, H. Matsueda, and

- Y. Sawa, 2012: Comparisons between XCH₄ from GOSAT shortwave and thermal infrared spectra and aircraft CH₄ measurements over Guam. *SOLA*, **8**, 145–149.
- Sawa, Y., T. Machida, and H. Matsueda, 2008: Seasonal variations of CO₂ near the tropopause observed by commercial aircraft. *J. Geophys. Res.*, **113**, D23301, doi:10.1029/2008JD010568.
- Sawa, Y., T. Machida, and H. Matsueda, 2012: Aircraft observation of the seasonal variation in the transport of CO₂ in the upper atmosphere. *J. Geophys. Res.*, **117**, D05305, doi:10.1029/2011JD016933.
- Sawa, Y., H. Matsueda, Y. Makino, H. Y. Inoue, S. Murayama, M. Hirota, Y. Tsutsumi, Y. Zaizen, M. Ikegami, and K. Okada, 2004: Aircraft observation of CO₂, CO, O₃ and H₂ over the North Pacific during the PACE-7 Campaign. *Tellus B*, **56**, 2–20.
- Sawa, Y., H. Tanimoto, S. Yonemura, H. Matsueda, A. Wada, S. Taguchi, T. Hayasaka, H. Tsuruta, Y. Tohjima, H. Mukai, N. Kikuchi, S. Katagiri, and K. Tsuboi, 2007: Widespread pollution events of carbon monoxide observed over the western North Pacific during the East Asian Regional Experiment (EAREX) 2005 campaign. *J. Geophys. Res.*, **112**, D22S26, doi:10.1029/2006JD008055.
- Schuck, T. J., K. Ishijima, P. K. Patra, A. K. Baker, T. Machida, H. Matsueda, Y. Sawa, T. Umezawa, C. A. M. Brenninkmeijer, and J. Lelieveld, 2012: Distribution of methane in the tropical upper troposphere measured by CARIBIC and CONTRAIL aircraft. *J. Geophys. Res.*, **117**, D19304, doi:10.1029/2012JD018199.
- Shirai, T., T. Machida, H. Matsueda, Y. Sawa, Y. Niwa, S. Maksyutov, and K. Higuchi, 2012: Relative contribution of transport/surface flux to the seasonal vertical synoptic CO₂ variability in the troposphere over Narita. *Tellus B*, **64**, 19138.
- Streets, D. G., T. C. Bond, G. R. Carmichael, S. D. Fernandes, Q. Fu, D. He, Z. Klimont, S. M. Nelson, N. Y. Tsai, M. Q. Wang, J.-H. Woo, and K. F. Yarber, 2003: An inventory of gaseous and primary aerosol emissions in Asia in the year 2000. *J. Geophys. Res.*, **108**, 8809, doi:10.1029/2002JD003093.
- Suntharalingam, P., D. J. Jacob, P. I. Palmer, J. A. Logan, R. M. Yantosca, Y. Xiao, M. J. Evans, D. G. Streets, S. L. Vay, and G. W. Sachse, 2004: Improved quantification of Chinese carbon fluxes using CO₂/CO correlations in Asian outflow. *J. Geophys. Res.*, **109**, D18S18, doi:10.1029/2003JD004362.
- Tanimoto, H., Y. Sawa, S. Yonemura, K. Yumimoto, H. Matsueda, I. Uno, T. Hayasaka, H. Mukai, Y. Tohjima, K. Tsuboi, and L. Zhang, 2008: Diagnosing recent CO emissions and ozone evolution in East Asia using coordinated surface observations, adjoint inverse modeling, and MOPITT satellite data. *Atoms. Chem. Phys.*, **8**, 3867–3880.
- Terao, Y., H. Mukai, Y. Nojiri, T. Machida, Y. Tohjima, T. Saeki, and S. Maksyutov, 2011: Interannual variability and trends in atmospheric methane over the western Pacific from 1994 to 2010. *J. Geophys. Res.*, **116**, D14303, doi:10.1029/2010JD015467.
- Tohjima, Y., T. Machida, M. Utiyama, M. Katsumata, Y. Fujimura, and S. Maksyutov, 2002: Analysis and presentation of in situ atmospheric methane measurements from Cape Ochi-ishi and Hateruma Island. *J. Geophys. Res.*, **107**, 4148, doi:10.1029/2001JD001003.
- Tohjima, Y., H. Mukai, S. Hashimoto, and P. K. Patra, 2010: Increasing synoptic scale variability in atmospheric CO₂ at Hateruma Island associated with increasing East-Asian emissions. *Atoms. Chem. Phys.*, **10**, 453–462.
- Tohjima, Y., H. Mukai, T. Machida, Y. Nojiri, and M. Gloor, 2005: First measurements of the latitudinal atmospheric O₂ and CO₂ distributions across the western Pacific. *Geophys. Res. Lett.*, **32**, L17805, doi:10.1029/2005GL023311.
- Tsuboi, K., H. Matsueda, Y. Sawa, Y. Niwa, M. Nakamura, D. Kuboike, K. Saito, H. Ohmori, S. Iwatsubo, H. Nishi, Y. Hanamiya, K. Tsuji, and Y. Baba, 2013: Evaluation of a new JMA aircraft flask sampling system and laboratory trace gas analysis system. *Atmos. Meas. Tech.*, **6**, 1257–1270.
- Turnbull, J. C., P. P. Tans, S. J. Lehman, D. Baker, T. J. Conway, Y. S. Chung, J. Gregg, J. B. Miller, J. R. Southon, and L.-X. Zhou, 2011: Atmospheric observations of carbon monoxide and fossil fuel CO₂ emissions from East Asia. *J. Geophys. Res.*, **116**, D24306, doi:10.1029/2011JD016691.
- Umezawa, T., T. Machida, K. Ishijima, H. Matsueda, Y. Sawa, P. K. Patra, S. Aoki, and T. Nakazawa, 2012: Carbon and hydrogen isotopic ratios of atmospheric methane in the upper troposphere over the Western Pacific. *Atoms. Chem. Phys.*, **12**, 8095–8113.
- Wada, A., H. Matsueda, Y. Sawa, K. Tsuboi, and S. Okubo, 2011: Seasonal variation of enhancement ratios of trace gases observed over 10 years in the western North Pacific. *Atmos. Environ.*, **45**, 2129–2137.
- Wada, A., Y. Sawa, H. Matsueda, S. Taguchi, S. Murayama, S. Okubo, and Y. Tsutsumi, 2007: Influence of continental air mass transport on atmospheric CO₂ in the western North Pacific. *J. Geophys. Res.*, **112**, D07311, doi:10.1029/2006JD007552.
- van der Werf, G. R., J. T. Randerson, L. Giglio, G. J. Collatz, M. Mu, P. S. Kasibhatla, D. C. Morton, R. S. DeFries, Y. Jin, and T. T. van Leeuwen, 2010: Global fire emissions and the contribution of deforestation, savanna, forest, agricultural, and peat fires (1997–2009). *Atoms. Chem. Phys.*, **10**, 11707–11735.
- Xiao, Y., D. J. Jacob, J. S. Wang, J. A. Logan, P. I. Palmer, P. Suntharalingam, R. M. Yantosca, G. W. Sachse, D. R. Blake, and D. G. Streets, 2004: Constraints on Asian and European sources of methane from CH₄-C₂H₆-CO correlations in Asian outflow. *J. Geophys. Res.*, **109**,

- D15S16, doi:10.1029/2003JD004475.
- Yashiro, H., S. Sugawara, K. Sudo, S. Aoki, and T. Nakazawa, 2009: Temporal and spatial variations of carbon monoxide over the western part of the Pacific Ocean. *J. Geophys. Res.*, **114**, D08305, doi:10.1029/2008JD010876.
- Zhao, C. L., and P. P. Tans, 2006: Estimating uncertainty of the WMO mole fraction scale for carbon dioxide in air. *J. Geophys. Res.*, **111**, D08S09, doi:10.1029/2005JD006003.
- Zhou, L., J. Tang, Y. Wen, P. Yan, J. Li, and X. Zhang, 2003: The impact of local winds and long-range transport on the continuous carbon dioxide record at Mount Waliguan, China. *Tellus B*, **55**, 145–158.
- Zhou, L., D. E. J. Worthy, P. M. Lang, M. K. Ernst, X. C. Zhang, Y. P. Wen, and J. L. Li, 2004: Ten years of atmospheric methane observations at a high elevation site in Western China. *Atmos. Environ.*, **38**, 7041–7054.
- Zhu, C., H. Yoshikawa-Inoue, H. Matsueda, Y. Sawa, Y. Niwa, A. Wada, and H. Tanimoto, 2012: Influence of Asian outflow on Rishiri Island, northernmost Japan: Application of radon as a tracer for characterizing fetch regions and evaluating a global 3D model. *Atmos. Environ.*, **50**, 174–181.